

## VALIDATION OF A NUMERICAL AND ANALYTICAL MODEL OF IMPACTED COLUMNS BY MEANS OF SMALL-SCALE DROP WEIGHT EXPERIMENTS

Carles Colomer Segura<sup>1</sup>, Nils Horbach<sup>1</sup> and Prof. Dr.-Ing Markus Feldmann<sup>1</sup>

<sup>1</sup>Institute of Steel Construction and Lightweight Construction  
RWTH Aachen University  
Mies-van-der-Rohe-Str. 1, 52074 Aachen, Germany  
e-mail: carles.colomer@rwth-live.de

**Keywords:** Impact of Columns, Simplified Model, Membrane Effects, Structural Dynamics, Drop Weight, Experiment, Validation

**Abstract.** *The analysis of structures under extreme accidental actions such as explosion or impact has been an ongoing topic of research since the 50's. Especially regarding the dynamic behaviour of impulsively loaded columns, many analytical and numerical models have been developed, which aim at predicting the ultimate load bearing capacity of the column and its residual level of deformation, which is directly linked to the residual capacity of the column after the impact.*

*Nevertheless most of the existing approaches lack an appropriate consideration of membrane related resisting mechanisms, either by completely neglecting the presence of any longitudinal restraints or by assuming them as perfectly rigid. A realistic evaluation of the dynamic behaviour of the column requires therefore a more exact approach in order to consider arbitrary longitudinal connector stiffnesses. This paper presents a new analytical approach to the deformational and energetic behaviour of impacted column elements, which allows for an closed form solution of the maximum displacements under arbitrary longitudinal boundary conditions.*

*On the other hand, a small-scale drop weight tower has been constructed in order to validate the results of the analytical model and compare them to predictions of other numerical approaches. The test rig has been conceived to allow for longitudinal displacements of the specimen, thus allowing to measure the motion of the column both in transversal and longitudinal direction.*

## 1 INTRODUCTION

The ability to predict the real damage of impulsively loaded columns is of major importance, as their failure might affect the structural integrity of the whole building. While at the early stages all investigations were based on analytical models [1, 2] (mostly consisting of the reduction of the column to a single degree of freedom system), the advent of the finite element method and the great increase in computer power of the latest decades has allowed engineers to simulate complex loading scenarios of columns in more and more realistic building environments. Nowadays, many investigations [3, 4, 5] focusing on detailed aspects of the behaviour are based on complex FEM. Nevertheless, for general design recommendations, the interest remains on the global behaviour of the column (Will it fail or not? How much will it deform?), where simplified design methods are still a very useful tool [6, 7].

Most of these simplified design methods are based on energetic considerations, where the bearing capacity of the column is limited by the amount of strain energy that can be absorbed by the column undergoing deformation due to the impact. At small displacements, the absorbed strain energy is purely related to the bending resistance of the column. Nevertheless, at higher displacement levels (to be expected in accidental events) the energy absorption capability of the column is dominated by its membrane behaviour and the absorbed longitudinal strain energy. Very often, this latter term is simplified or even neglected in most analytical formulations, because of its complexity due to the nonlinear dependence on the displacements, thus leading to analytical models that underestimate the true energy absorbing capabilities of the column.

At the Institute of Steel Structures of the RWTH Aachen, exact analytical models have been developed, which can exactly assess the energy absorption capabilities of columns both due to bending and membrane effects under consideration of arbitrary longitudinal boundary conditions [8, 9].

In a first stage (Chapter 2), the longitudinal deformation behaviour of a beam undergoing arbitrary transversal deformation will be investigated. This will allow to describe the coupled (transversal-longitudinal) behaviour of the beam with increasing transversal deformation and thus understand the combined energy absorption mechanisms (bending-membrane) happening during the deformation process. In Chapter 3, an analytical solution of the energy absorption capability of the beam due to bending and membrane at any level of deformation will be given.

In order to validate this model, a small-scale experimental weight drop set-up (Chapter 4) has been constructed and used to impact small beam elements under variation of mechanical boundary conditions.

Using imaging measuring techniques, as well as optical laser displacement transducers and accelerometers, the experimental set-up allows for very detailed investigations of the applied impact energy and the deformational response of the specimen. These results are used in Chapter 5 to validate the analytical model in two experiments with free and fixed longitudinal boundary conditions.

## 2 CONSIDERATION OF GEOMETRIC NONLINEAR EFFECTS IN AN ARBITRARILY DEFORMED BEAM

Under consideration of geometric nonlinearities, transversal displacements lead to longitudinal displacements and/or activation of membrane forces along the beam. A proper

analysis of the energetic behaviour of the beam including geometric nonlinear effects requires the analytical determination of the longitudinal deformation function  $\Upsilon_2(s, t)$ , related to an arbitrary deflection function  $\Psi(s, t)$  and arbitrary boundary conditions in longitudinal direction as in figure 1.

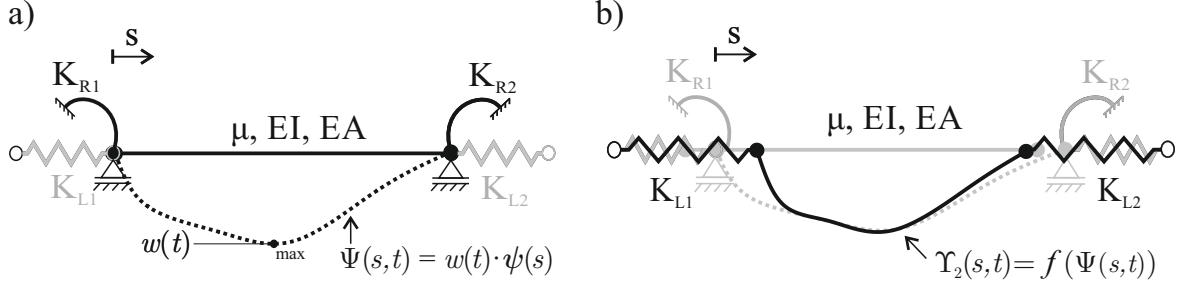


Figure 1: Arbitrary deformation of a beam in transversal direction (a) and associated deformation in longitudinal direction due to geometric nonlinear effects (b)

For the consideration of geometric nonlinear effects along the beam, the following geometric nonlinear strain definition is used:

$$\varepsilon_2 = \frac{\partial \Upsilon_2}{\partial s} + \frac{1}{2} \left( \frac{\partial \Psi}{\partial s} \right)^2 \quad (1)$$

where  $\varepsilon_2$  represents the axial stretching of the beam due to a transversal deflection  $\Psi(s, t)$ , which is calculated as the difference between the shortening under no axial restraintment  $\frac{1}{2} \left( \frac{\partial \Psi}{\partial s} \right)^2$  and the actual shortening including the spring stiffnesses of the longitudinal supports ( $k_{L1}$ ,  $k_{L2}$ ) and axial beam stiffness ( $k_{EA} = EA/L$ ). For the upcoming analysis, it is useful to define the non-dimensional spring stiffnesses:

$$k_{L1}^* = k_{L1}/k_{EA} \quad \text{and} \quad k_{L2}^* = k_{L2}/k_{EA} \quad .$$

Assuming that the axial force remains constant along the entire length of the beam, the

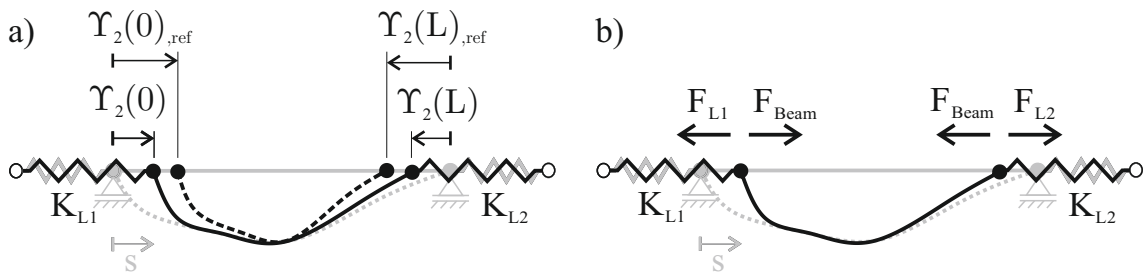


Figure 2: Longitudinal deformation of a beam due to geometrical nonlinear effects (a) and equilibrium of longitudinal forces (b)

axial stretching of the beam can be easily calculated by integrating eq. (1) over the beam length:

$$\varepsilon_2 = \frac{\Upsilon_2(L) - \Upsilon_2(0)}{L} + \frac{1}{2L} \int_0^L \left( \frac{\partial \Psi}{\partial s} \right)^2 \quad (2)$$

In order to determine the longitudinal displacement of the left and right supports ( $\Upsilon_2(0)$  and  $\Upsilon_2(L)$  respectively), the equilibrium of axial forces in the system depicted in figure 2 b) is imposed, leading to the following linear system of equations:

$$\left. \begin{aligned} F_{L1} = F_{Beam} \rightarrow k_{L1}\Upsilon_2(0) &= \frac{EA(\Upsilon_2(L) - \Upsilon_2(0))}{L} + \frac{EA}{2L} \int_0^L \left( \frac{\partial \Psi}{\partial s} \right)^2 ds \\ -F_{L2} = F_{Beam} \rightarrow -k_{L2}\Upsilon_2(L) &= \frac{EA(\Upsilon_2(L) - \Upsilon_2(0))}{L} + \frac{EA}{2L} \int_0^L \left( \frac{\partial \Psi}{\partial s} \right)^2 ds \end{aligned} \right\} \quad (3)$$

The solution for  $\Upsilon_2(0)$  and  $\Upsilon_2(L)$  from eq. (3) can be found to:

$$\left. \begin{aligned} \Upsilon_2(0) &= \frac{k_{1eq}}{2} \int_0^L \left( \frac{\partial \Psi}{\partial s} \right)^2 ds \\ \Upsilon_2(L) &= \frac{-k_{2eq}}{2} \int_0^L \left( \frac{\partial \Psi}{\partial s} \right)^2 ds \end{aligned} \right\} \quad (4)$$

with

$$k_{1eq} = k_{L2}^* / (k_{L1}^* \cdot k_{L2}^* + k_{L1}^* + k_{L2}^*) \quad (5)$$

$$k_{2eq} = k_{L1}^* / (k_{L1}^* \cdot k_{L2}^* + k_{L1}^* + k_{L2}^*) \quad (6)$$

From here, the overall shortening of the beam  $\Delta\Upsilon_{2,1 \rightarrow L}$  can be defined as:

$$\Delta\Upsilon_{2,0 \rightarrow L} = \Upsilon_2(0) - \Upsilon_2(L) = \frac{k_{1,eq} + k_{2,eq}}{2} \int_0^L \left( \frac{\partial \Psi}{\partial s} \right)^2 ds \quad (7)$$

The non-dimensional spring stiffnesses ( $k_{1,eq}$ ,  $k_{2,eq}$ ) range from (0,0) for a fixed-fixed restraint to (0,1) for a fixed-free situation. In case of no longitudinal restraint ( $k_{L1} = 0$  and  $k_{L2} = 0$ ), the values of ( $k_{1,eq}$ ,  $k_{2,eq}$ ) are equal to (0.5,0.5) and lead to a symmetrical shortening of the beam. The values of ( $k_{1,eq}$ ,  $k_{2,eq}$ ) can be determined according to figure 3.

From a mechanical point of view, the axial force in the beam for any longitudinal boundary condition where  $k_{1,eq} + k_{2,eq} = 1$  (either free-fixed, fixed-free or free-free conditions for the springs  $K_{L1}$  and  $K_{L2}$ ) must be equal to 0 due to force equilibrium along the beam axis. In this situations, eq. (7) yields:

$$\Delta\Upsilon_{2,0 \rightarrow L,ref} = \frac{1}{2} \int_0^L \left( \frac{\partial \Psi}{\partial s} \right)^2 ds \quad (8)$$

which is defined as the reference overall shortening for which no axial forces are developed and hence, no strain membrane energy is absorbed by the system.

In the general case of a horizontally restrained beam, the overall shortening of the beam  $\Delta\Upsilon_{2,0 \rightarrow L}$  is always smaller than  $\Delta\Upsilon_{2,0 \rightarrow L,ref}$ , leading to the development of membrane forces. In this state, the axial stretching of the beam is calculated from eq. (2) to:

$$\varepsilon_2 = \frac{(\Delta\Upsilon_{2,0 \rightarrow L,ref} - \Delta\Upsilon_{2,0 \rightarrow L})}{L} = \frac{1 - k_{1,eq} - k_{2,eq}}{2L} \int_0^L \left( \frac{\partial \Psi}{\partial s} \right)^2 ds \quad (9)$$

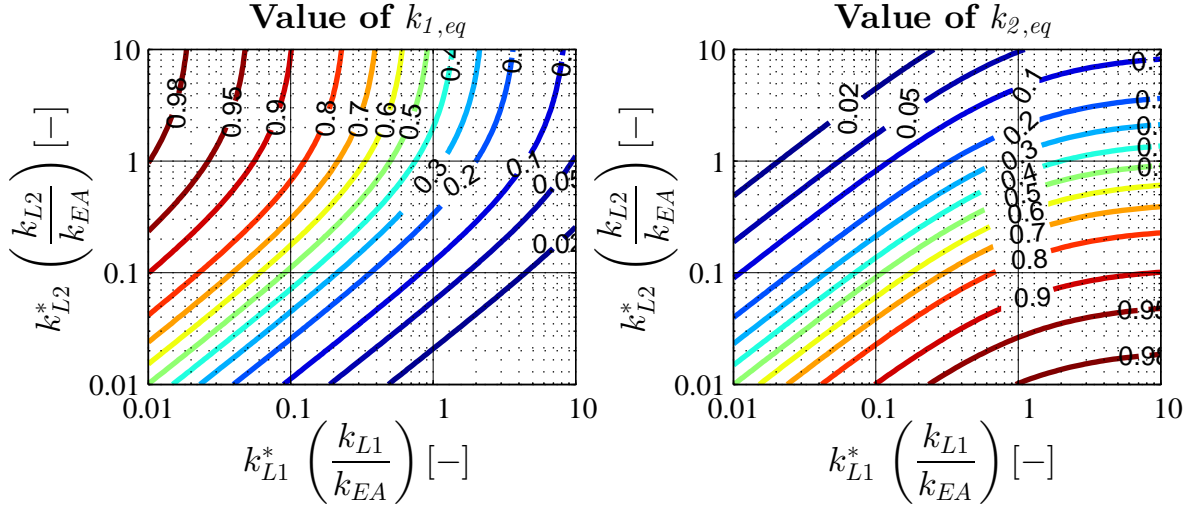


Figure 3: Non-dimensional spring stiffnesses for arbitrary longitudinal boundary conditions

which is always positive as membrane forces can only be positive.

In this state, the deformations of the beam in longitudinal direction can be calculated from eqs. (1) and (9) to:

$$\frac{\partial \Upsilon_2}{\partial s} = \varepsilon_2 - \frac{1}{2} \left( \frac{\partial \Psi}{\partial s} \right)^2 = \frac{1 - k_{1,eq} - k_{2,eq}}{2L} \int_0^L \left( \frac{\partial \Psi}{\partial s} \right)^2 ds - \frac{1}{2} \left( \frac{\partial \Psi}{\partial s} \right)^2 \quad (10)$$

which integrated along the beam axis and imposing the boundary conditions in (4) yields:

$$\begin{aligned} \Upsilon_2(s, t) &= \frac{s - k_{1,eq}(s - L) - k_{2,eq} \cdot s}{2L} \int_0^L \left( \frac{\partial \Psi}{\partial s} \right)^2 ds - \frac{1}{2} \int_0^s \left( \frac{\partial \Psi}{\partial s} \right)^2 ds = \\ &= \left( \frac{s - k_{1,eq}(s - L) - k_{2,eq} \cdot s}{2L} \int_0^L \left( \frac{\partial \psi}{\partial s} \right)^2 ds - \frac{1}{2} \int_0^s \left( \frac{\partial \psi}{\partial s} \right)^2 ds \right) \cdot w(t)^2 \end{aligned} \quad (11)$$

This expression describes the longitudinal displacements of a beam due to an arbitrary transversal deformation under consideration of geometric nonlinear effects and arbitrary longitudinal support stiffnesses.

By defining the following functional:

$$f_{\Upsilon_2}(s) = \left( \frac{s - k_{1,eq}(s - L) - k_{2,eq} \cdot s}{2L} \int_0^L \left( \frac{\partial \psi}{\partial s} \right)^2 ds - \frac{1}{2} \int_0^s \left( \frac{\partial \psi}{\partial s} \right)^2 ds \right) \quad (12)$$

eq. 11 can be rewritten as:

$$\Upsilon_2(s, t) = f_{\Upsilon_2}(s) \cdot w(t)^2 \quad (13)$$

### 3 ENERGY ABSORPTION CAPABILITY OF A COLUMN UNDER CONSIDERATION OF MEMBRANE ACTION

The strain energy absorbed by a beam undergoing a deformation as defined in figure 1 can be calculated by integral calculation over the length of the beam as:

$$E_{\varepsilon^*, S} = E_{\varepsilon, S} + E_{\kappa, S} = \frac{1}{2} \int EA \cdot \varepsilon^2 \cdot ds + \frac{1}{2} \int EI \cdot \kappa^2 \cdot ds \quad (14)$$

where the terms  $E_{\varepsilon,S}$  and  $E_{\kappa,S}$  correspond to the absorbed energy components due to membrane and bending action respectively. For a correct evaluation of the absorbed energy, the boundary conditions need to be considered in the evaluation of these integrals. Thus, the general expression for the calculation of the absorbed strain energy due to bending and membrane action become respectively:

$$E_{\kappa,S} = \frac{1}{2} \left[ \int EI \left( \frac{\partial^2 \psi(s)}{\partial s^2} \right)^2 ds + k_{R1} \cdot \left( \frac{\partial \psi}{\partial s}(0) \right)^2 + k_{R2} \cdot \left( \frac{\partial \psi}{\partial s}(L) \right)^2 \right] \cdot w(t)^2 \quad (15)$$

$$E_{\varepsilon,S} = \frac{1}{2} \left[ \int EA \cdot \varepsilon^2 \cdot ds + k_{L1} \cdot \Upsilon(0)^2 + k_{L2} \cdot \Upsilon(L)^2 \right] \quad (16)$$

with the help of the eqs. (9) and (4) as well as the definitions of  $k_{1,eq}$  and  $k_{2,eq}$  from eqs. (5) and (6), eq. (16) can be rewritten as:

$$E_{\varepsilon,S} = \frac{k_{EA} k_{L1}^* k_{L2}^*}{8 (k_{L1}^* + k_{L2}^* + k_{L1}^* \cdot k_{L2}^*)} \left( \int_0^L \left( \frac{\partial \psi}{\partial s} \right)^2 ds \right)^2 \cdot w(t)^4 \quad (17)$$

This last expression shows the nonlinear dependency of the absorbed membrane energy as a function of the transversal deformation  $w(t)$ .

Fur the upcoming analysis, eq. (14) will be rewritten as

$$E_{\varepsilon^*,S} = C_{\kappa,w^2} \cdot w^2 + C_{\varepsilon,w^4} \cdot w^4 \quad (18)$$

with

$$C_{\kappa,w^2} = \frac{1}{2} \left[ \int EI \left( \frac{\partial^2 \psi(s)}{\partial s^2} \right)^2 ds + k_{R1} \cdot \left( \frac{\partial \psi}{\partial s}(0) \right)^2 + k_{R2} \cdot \left( \frac{\partial \psi}{\partial s}(L) \right)^2 \right] \quad (19)$$

$$C_{\varepsilon,w^4} = \frac{k_{EA} k_{L1}^* k_{L2}^*}{8 (k_{L1}^* + k_{L2}^* + k_{L1}^* \cdot k_{L2}^*)} \left( \int_0^L \left( \frac{\partial \psi}{\partial s} \right)^2 ds \right)^2 \quad (20)$$

where  $C_{\kappa,w^2}$  and  $C_{\varepsilon,w^4}$  are coefficients purely dependent on the deformation shape and boundary conditions and  $w$  is the amplitude of the transversal deformation.

### 3.1 Consideration of the plastic development in the column

In problems where large deformation levels are expected, it is important to take into account the development of plastic hinges during the deformation of the column (as in figure 4). With increasing transversal deformation  $w$  new plastic hinges appear, which lead to changes in the deformation shape  $\psi(s)$ . This means that the eq. (18) is only valid for a given deformation interval, in which the deformation shape  $\psi$  remains constant. Therefore, this equation should be more correctly be written in its incremental form for a given stage  $i$  in the plastic evolution of the beam:

$$\Delta E_{\varepsilon^*,S,w_i \rightarrow w} = C_{\kappa,w^2,i} \cdot (w - w_i)^2 + C_{\varepsilon,w^4,i} \cdot (w^2 - w_i^2)^2 \quad (21)$$

It is important to note, that the expression (21) does not consider the energy contribution due to the remaining plastic resistance from the previous stages of the plastic evolution of

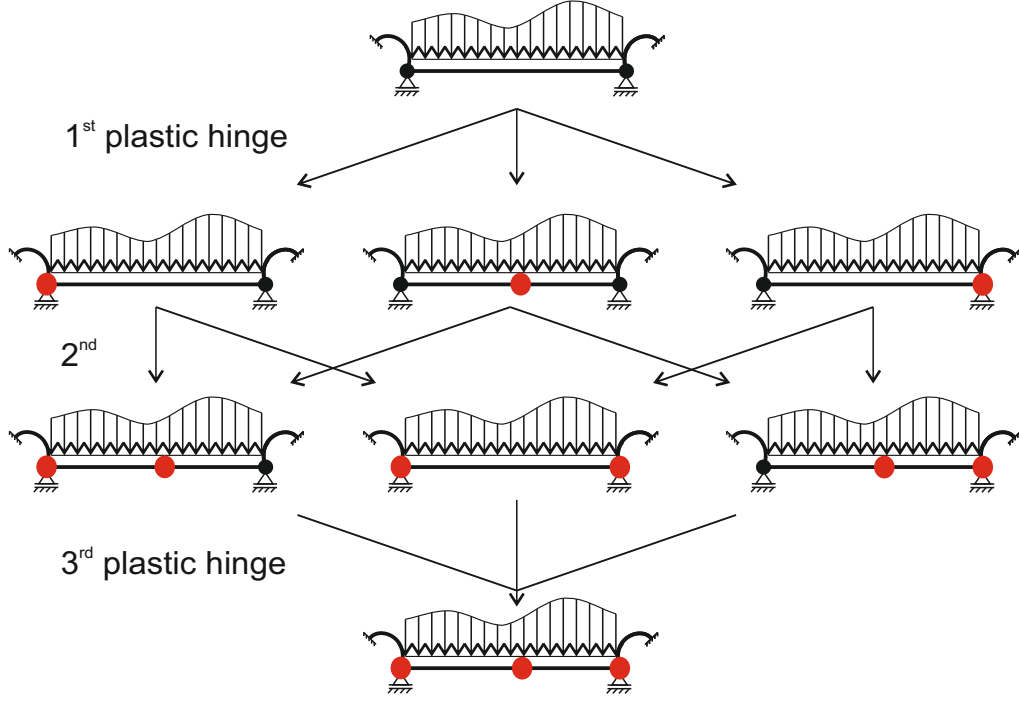


Figure 4: Plastic evolution of an arbitrarily supported beam

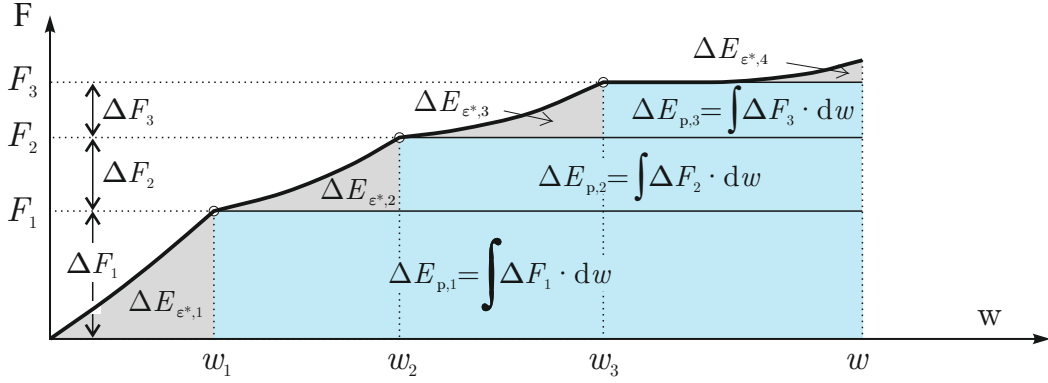


Figure 5: Generalized Force-Displacement diagram of a plastic beam and integration areas for the determination of the totally absorbed energy

the beam. In order to account for this components, additional integral terms  $\Delta E_{p,i}$  need to be considered in the calculation of the total energy, as illustrated in figure 5. If the deflections  $w_i$  are known from the plastic analysis, the only remaining unknown terms are the force increments between plastic stages  $\Delta F_i$ , which can be calculated derivating eq. (21):

$$\Delta F_i = \frac{\partial \Delta E_{\varepsilon^*, S, w_{i-1} \rightarrow w_i}}{\partial w} = 2 \cdot C_{\kappa, w^2, i} \cdot (w_i - w_{i-1}) + 4 \cdot C_{\varepsilon, w^4, i} \cdot (w_i^2 - w_{i-1}^2) \cdot w \quad (22)$$

The plastic energy components  $\Delta E_{p,i}$  can be calculated using eq. (22) to:

$$\Delta E_{p,i} = \int_{w_i}^w \Delta F_i \cdot dw = 2 \cdot C_{\kappa, w^2, i} \cdot (w_i - w_{i-1}) \cdot (w - w_i) + 4 \cdot C_{\varepsilon, w^4, i} \cdot (w_i^2 - w_{i-1}^2) \cdot (w^2 - w_i^2) \quad (23)$$

## 4 EXPERIMENTAL INVESTIGATIONS

### 4.1 Testing set-up

In order to perform impact experiments, a small-scale impact test facility has been constructed at the Institute of Steel Construction of the RWTH Aachen (see figure 6). Using the inner flange of a building column as a support for the guide-rails of the drop tower. The maximum drop height is limited to 2.5 metres, with a weight of the impact console of 2.8 kg, which can be increased modularly upto 10 kg. The applicable impact energy can reach upto  $\sim 250$  J with a maximum impact speed of 7.0 m/s.

As illustrated in figure 6, the test rig for impacting steel plates has been designed to allow for adjusting the rotatory and longitudinal boundary conditions arbitrarily. Directly attached to a 20mm thick steel base plate, there is a guiding rail with a length of  $\sim 1840$  mm supporting two runner blocks. In order to allow for high levels of deformation in the test specimen, a stiff support structure has been constructed to elevate the impact point of the specimen from the longitudinal rail, thus allowing for a free transverse deformation of max. 20 cm.

Two roll bearings bolted to the support structure hold an 30 x 30 mm square axle with a 10 mm wide mill-cut slot where the test specimen is introduced and fixed by clamping. The maximum size of the test specimen is limited to 1650 x 200 x 10 mm. The measuring

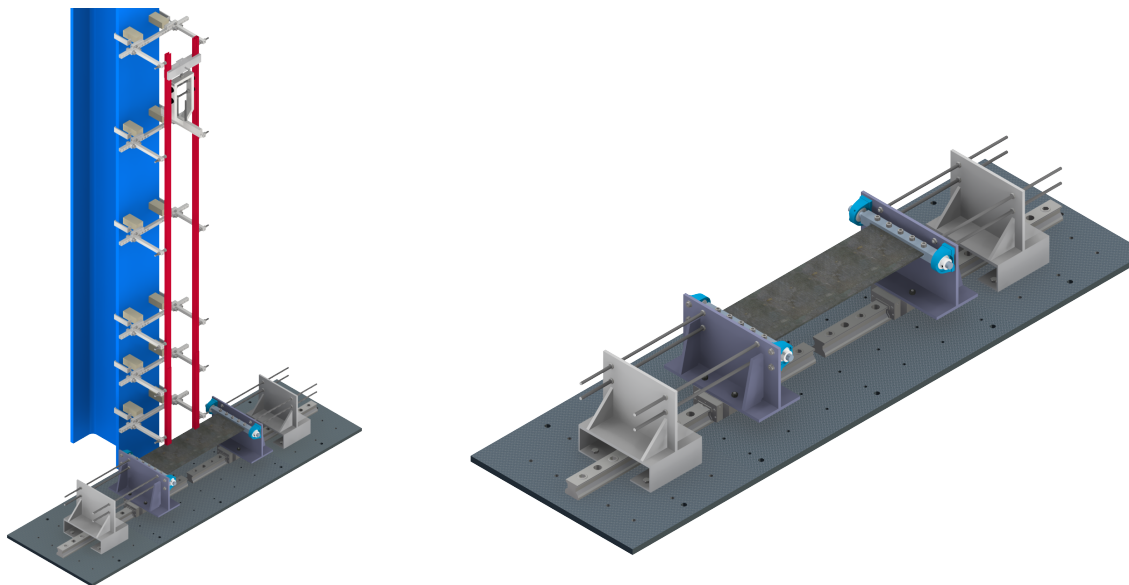


Figure 6: Overview of the small-scale drop weight tower (a) and detail of the test rig for impacting small scale specimens (b)

system for the experimental set-up is composed by:

1. An accelerometer attached to the impact console for measuring the impact force.
2. Two high-speed cameras with a resolution of 1024 x 512 pixel at 923 fps, in combination with Tracker software [10], a free video analysis tool built on the Open Source Physics Java framework.



## 4.2 Planned experiments

The goal of the experiments described in figure 7 is to validate the analytical approaches presented in the Chapters 2 and 3 regarding the geometrical nonlinear behaviour and the associated energy absorbing mechanisms of impacted columns by means of small scale experiments.

In the test configuration (a), a simply supported plate with the dimensions 500 x 110x 3 mm was tested under free-free rotary and free-free longitudinal boundary conditions. In the test configuration (b), the longitudinal boundary conditions have been set to fixed-fixed, in order to activate membrane effects. In both experiments, an impact mass of 2.8 kg has been raised to a height of 1.82 m and let fall freely against the middle of the specimen, thus applying an impact energy of  $\sim 50$  J.

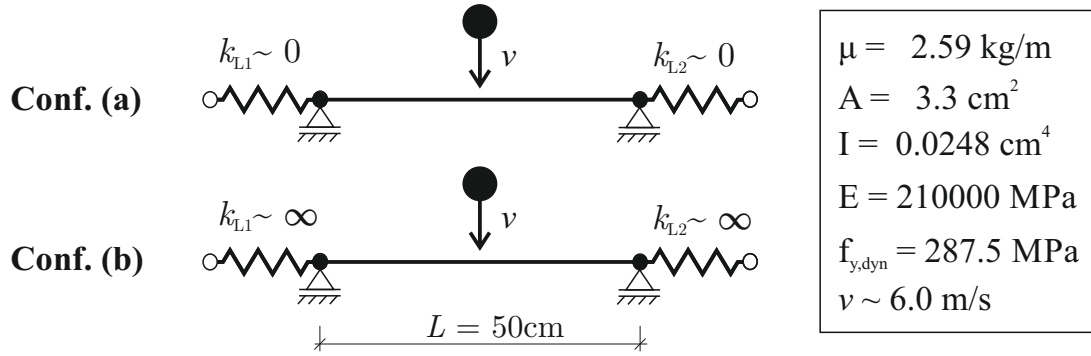


Figure 7: Boundary conditions for the performed experiments

## 5 EXPERIMENTAL RESULTS AND VALIDATION OF THE MODEL

In this chapter the results of the experimental tests are compared to the results of the analytical approach described in chapter 3 and also compared to the results of a numerical approach based on the model reduction concept specially designed for accounting for membrane effects [9]. The analytical approach allows for the estimation of the maximum

Load									
	Stage	BC's	$C_{\kappa, W^2}$	BC's	$C_{\varepsilon, W^4}$	BC's	$C_{\varepsilon, W^4}$	Limits	$W_i^*$
	1	$k_{R1}^*$	9979	$k_{L1}^*$	0	$k_{L1}^*$	1.71e7		0
	2	$\infty$	0	0	0	$\infty$	1.19e7		0.0285
	3	$k_{R2}^*$	-	$k_{L2}^*$	-	$k_{L2}^*$	-		-
	4	$\infty$	-	0	-	$\infty$	-		-

Figure 8: Values of the coefficients of the coefficients  $C_{\kappa, w^2, i}$  and  $C_{\varepsilon, w^4, i}$  for the boundary conditions in the experiments

deflections of the beam based on the determination of the coefficients  $C_{\kappa, w^2, i}$  and  $C_{\varepsilon, w^4, i}$  for each stage of the plastic evolution of the beam as described in figure 4. Since there are

no rotational supports at both ends, only the elastic (1) and perfectly plastic (2) stages are considered (see figure 8).

### 5.1 Experiment 1: Conf. (a)

The goal of this experiment was to investigate the behaviour of the beam under free-free longitudinal and rotationary boundary conditions. The measured deformational behaviour is shown in figure 12. In this situation, the only resistance mechanisms initially considered to absorb the impact energy are due to the bending deformation of the beam.

Using the analytical approach from chapter 3, it is possible to estimate the necessary deformation to absorb the impacting energy (50J) to 0.101 m. This result contradicts apparently the measurements and can only be explained if further attention is paid to secondary effects that might contribute to the absorption of the impact energy. As it can be observed in figure 12, the lateral supports undergo a significant longitudinal displacement within a short a time. This effect, combined to the fact that the lateral supports have a mass of  $\sim 20$  kg each, lead to an unexpected absorption of part the impact energy through the lateral supports in form of kinetic energy (see figure 9) that was later dissipated by friction and thus, did not cause any additional transverse deflection.

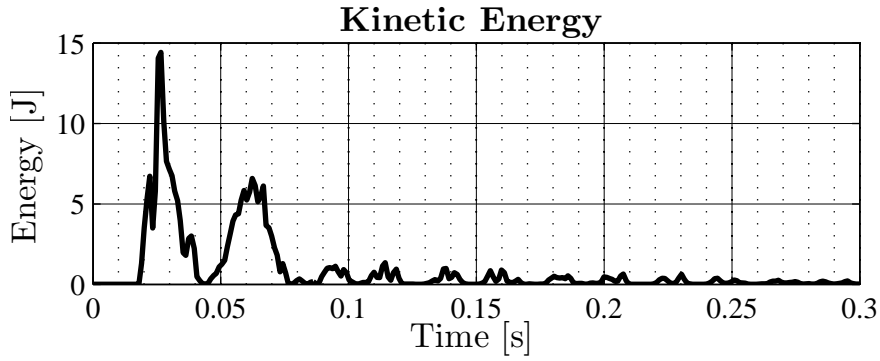


Figure 9: Evolution of the kinetic energy absorbed by the support construction due to its movement in longitudinal direction, Test Conf. (a)

Hence, the impact energy applied to the specimen is distributed into  $\sim 15$  J into the supports (and then dissipated by friction) and  $\sim 35$  J into the bending of the beam. In fact, figure 10 shows the energy absorption curve calculated for the system tested in Conf. (a). Here it is evident that the assumption of all impact energy being absorbed by the specimen leads to overestimating the transverse deflections, while the consideration of the kinetic lateral components leads to a much more accurate estimation of the maximum achieved deformation with a value of  $w_{\max} = 0.076\text{m}$ .

### 5.2 Experiment 2: Conf. (b)

The goal of this experiment was to investigate the behaviour of the beam under fixed-fixed longitudinal boundary conditions in order to validate the ability of the proposed analytical model to describe the energy absorbing mechanisms due to membrane action. The measured deformational behaviour is shown in figure 13. On the contrary to the tests in the Conf. (a), the only resistance mechanisms that can absorb the impact energy are related to the bending and longitudinal deformation of the beam. Here the lateral

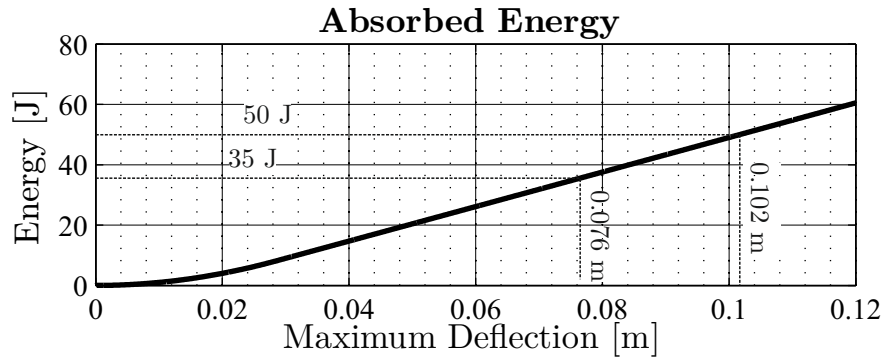


Figure 10: Energy absorption curve acc. to chapter 3 for Test Conf. (a)

supports are fixed and do not displace, thus they cannot absorb any kinetic energy.

Using the analytical approach explained in chapter 3, it is possible to estimate the necessary deformation to absorb the impacting energy (50J) to 0.036 m. This result agrees very well with the measurements shown in figure 13. As it can be observed in figure 11, the effects of the longitudinal restrain on the energy absorption capability of the specimen are of great importance and can be analytically described by the proposed model.

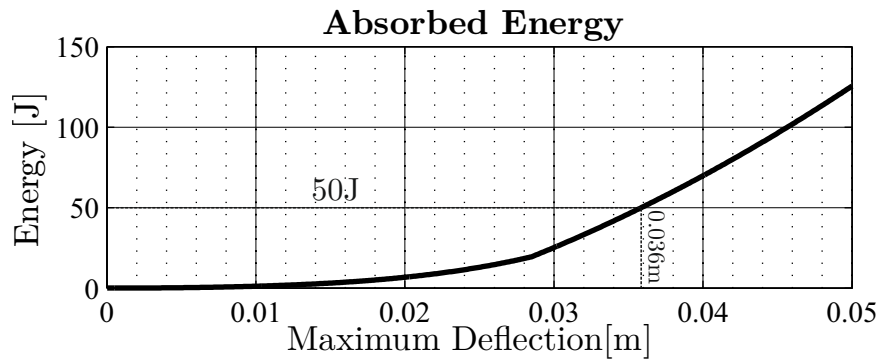


Figure 11: Energy absorption curve acc. to chapter 3 for Test Conf. (b)

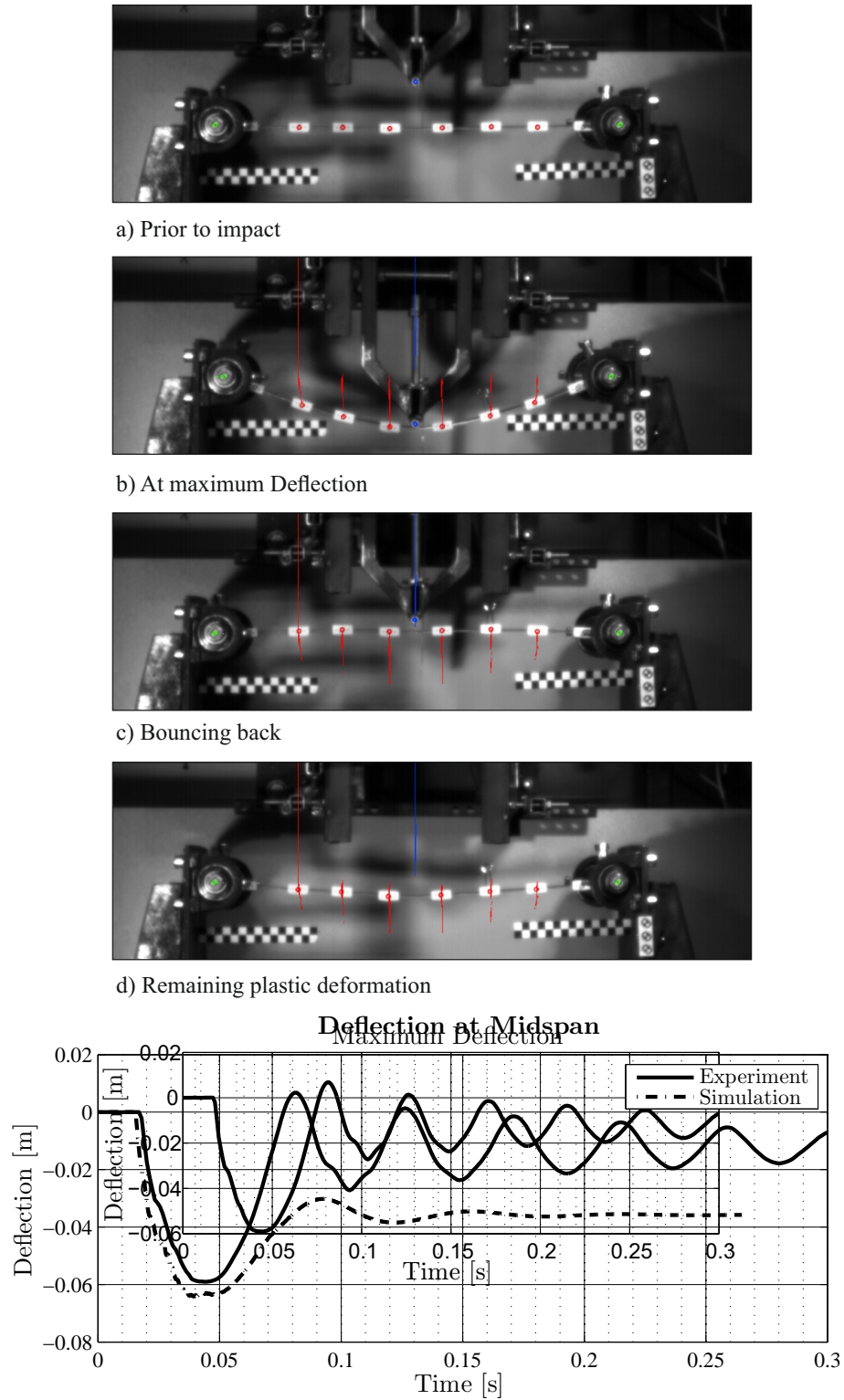
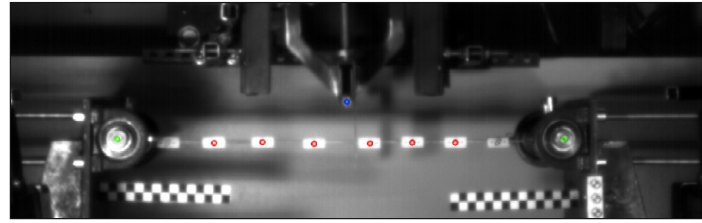
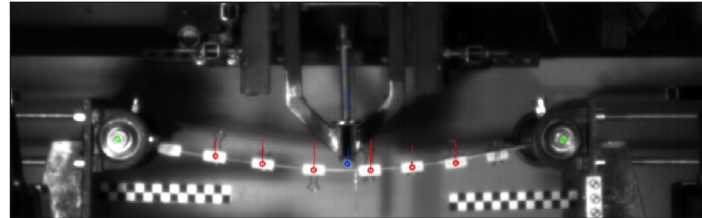


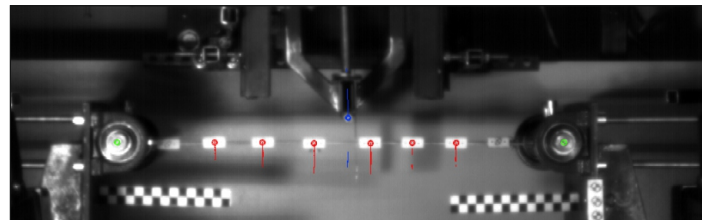
Figure 12: Evolution of the deformation during the impact test, Experiment and numerical Simulation, Test Conf. (a)



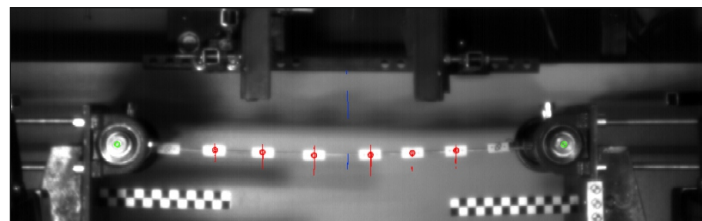
a) Prior to impact



b) At maximum Deflection



c) Bouncing back



d) Remaining plastic deformation

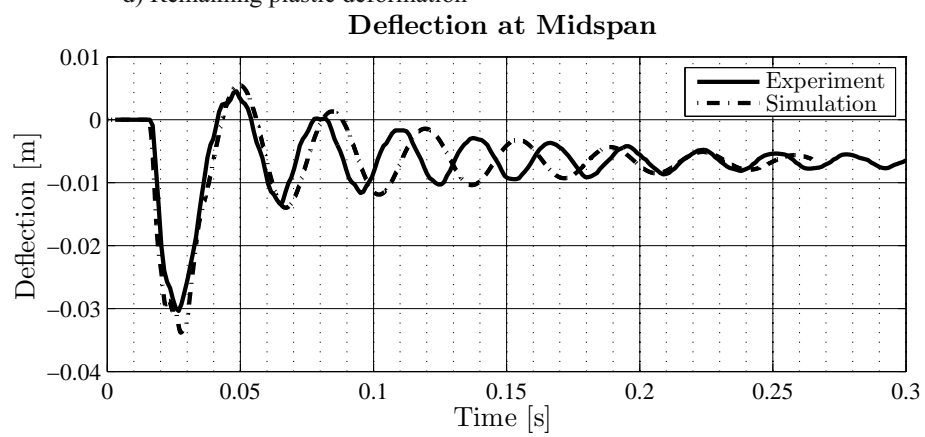


Figure 13: Evolution of the deformation during the impact test, Experiment and numerical Simulation, Test Conf. (b)

## 6 CONCLUSIONS

In this work, a new approach to the analytical determination of deformations of impacted columns has been presented and validated by means of experiments on a small-scale drop weight test rig.

The resistance behaviour of a column is dramatically increased if the membrane behaviour is taken into account in the energetic analysis of the column. This has been performed by considering a non-linear strain hypothesis, which lead to an additional energy absorption term dependent on the fourth power of the transversal displacement and the coefficient  $C_{\varepsilon,w^4}$ . Since the new analytical approach aims at describing the energy behaviour at large deformation levels, the evolution of the plastic stages has been included in the model, leading to a cumulative integration of the energy absorption function as described in chapter 3.1. This approach has been successfully validated by means of the experiment Conf. (b).

Another interesting fact could be observed during the performance of test Conf. (a). In a longitudinal unrestrained situation, the impact energy is partially transformed into kinetic energy by a longitudinal movement of the lateral supports. Real columns tend to have large head masses and thus, this becomes an interesting effect that should not remained unconsidered.

## REFERENCES

- [1] C.H. Norris, R.J. Hansen, M.J. Holley, J.M. Biggs, S. Namyet and J.K. Mianimi, *Structural Design for Dynamic Loads*, McGraw-Hill, New York, 1959.
- [2] J.M. Biggs, *Introduction to structural dynamics*, McGraw-Hill, New York, 1964.
- [3] M. Feyerabend, *Der harte Querstoß auf Stützen aus Stahl und Stahlbeton*, Univ. Karlsruhe, PhD, 1988.
- [4] , Klaus Willnow, *Stahlstützen unter räumlicher dynamischer Beanspruchung durch Anprall: Dissertation*, Ruhr-Universität Bochum, 1996.
- [5] H.A.B. Al-Thairy, Haitham Ali Bady, *Behaviour and design of steel columns subjected to vehicle impact*, University of Manchester, 2012.
- [6] Fire and Blast Information Group (FABIG), *Simplified methods for analysis of response to dynamic loading*, Steel Construction Institute, Technical Note, 2002.
- [7] *NORSOK standard N-004: Design of Steel Structures*, NORSOK, 2013
- [8] C. Colomer Segura and M. Feldmann, *A New Simplified Design Method for Steel Structures under Impulsive Loading*, WIT Transactions on the Built Environment, WIT-Press, Vol. 141, 2014.
- [9] C. Colomer Segura and M. Feldmann, *A New Model Reduction Technique to Predict the Effects of Blast Loading on Structures*, EUROODYN'2014 - 9th European Conference on Structural Dynamics, 2014.
- [10] D. Brown, Tracker Software, Open Source Physics (OSP) Project, [www.cabrillo.edu/~dbrown/tracker/](http://www.cabrillo.edu/~dbrown/tracker/)